Soft Matter

Dynamic Article Links

Cite this: *Soft Matter*, 2012, **8**, 8697

www.rsc.org/softmatter

PAPER

Colloidal gelation of oppositely charged particles†

Emily R. Russell,[a] Joris Sprakel,[bc] Thomas E. Kodger[c] and David A. Weitz*[ac]

Received 18th April 2012, Accepted 27th June 2012
DOI: 10.1039/c2sm25901j

Colloidal gelation has been extensively studied for the case of purely attractive systems, but little is understood about how colloidal gelation is affected by the presence of repulsive interactions. Here we demonstrate the gelation of a binary system of oppositely charged colloids, in which repulsive interactions compete with attractive interactions. We observe that gelation is controlled by varying the total volume fraction, the interaction strength, and the new tuning parameter of the mixing ratio of the two particle types, and present a state diagram of gelation along all these phase-space coordinates. Contrary to commonly studied purely attractive gels, in which weakly quenched gels are more compact and less tenuous, we find that particles in these binary gels form fewer contacts and the gels become more tenuous as we approach the gel point. This suggests that a different mechanism governs gel formation and ultimate structure in binary gelation: particles are unable to form additional favorable contacts through rearrangements, due to the competition of repulsive interactions between similarly charged colloids and attractive interactions between oppositely charged colloids.

1. Introduction

Colloidal gels are remarkable materials, their solid-like properties being determined primarily by a network of particles which make up a relatively small fraction of the total volume. The mechanisms controlling the formation and properties of colloidal gels offer interesting fundamental questions which have been extensively studied, and there is now a good understanding of how the formation and structure of purely attractive colloidal gels are governed by the particle volume fraction, depth of attraction, and range of interaction.[1–12] It is clear that the formation of a space-filling network at low volume fraction requires attractive interparticle interactions in order to form stress-supporting bonds between particles. Surprisingly, colloidal gelation can also take place in systems where repulsive interactions compete with attractive interactions.[13,14] Several examples of colloidal gels have been observed in binary suspensions of particles which carry opposite electric charges, in which repulsive interactions between similarly charged particles are present in addition to the attractive interactions between oppositely charged particles which drive gelation.[15–19] Such binary colloidal gels exhibit a rich behavior, yet the conditions under which they form, and the physical mechanisms governing their properties, are not yet well understood.

Here we introduce a new experimental model system which allows us to study the colloidal gelation of oppositely charged particles, and determine the state diagram describing the circumstances under which a gel forms. We demonstrate that the mixing ratio of the two particle types can be used as a tuning parameter, controlling the formation and structure of the gels. Unexpectedly, we find that unlike in purely attractive gels,[2,3] the number of contacts a particle forms in a binary gel decreases as we approach the transition to the fluid state; this decrease in contact number is invariant whether this gel line is approached by changing the interaction strength or by changing the mixing ratio. This suggests that screening of the charges, either through addition of small electrolyte ions, or through microscopically large macro-ions, is the main mechanism tuning the gelation process and final structure of the binary colloidal gels.

2. Experimental

Particles with a diameter of 2 μm are polymerized from *tert*-butyl methacrylate and trifluoro ethyl methacrylate,[20] a copolymer combination which permits both the refractive index and the density of the particles to be matched by a polar solvent mixture of formamide and sulfolane. Refractive index matching minimizes scattering of light by the particles, allowing us to visualize the interiors of bulk samples, and obtain precise information about the three-dimensional structure and dynamics of these gels, using confocal microscopy. Density matching minimizes the effects of buoyancy, which if present can dramatically alter the structure of a colloidal gel and the location of the gel line.[21] After synthesis, a single batch of seed particles is split in two portions; each portion is then fluorescently dyed, and given either a

[a]*Department of Physics, Harvard University, 17 Oxford St., Cambridge, MA 02138, USA. E-mail: weitz@seas.harvard.edu*
[b]*Laboratory of Physical Chemistry and Colloid Science, Wageningen University, Dreijenplein 6, 6703 HB Wageningen, The Netherlands*
[c]*School of Engineering and Applied Science, Harvard University, 29 Oxford St., Cambridge, MA 02138, USA*
† Electronic supplementary information (ESI) available. See DOI: 10.1039/c2sm25901j

positive or a negative electric charge by polymerizing a strong polyelectrolyte brush from initiators incorporated on the particle surface.[20] The positively charged brush is a random copolymer of cationic (3-acrylamidopropyl)trimethylammonium and neutral *N*,*N*-dimethylacrylamide, while the negatively charged brush is a copolymer of anionic 2-acrylamido-2-methyl-1-propanesulfonic acid with the same neutral monomer. Using the same seed batch for both the positively and negatively charged particles ensures that the two particle types have equal sizes and distributions. Two different fluorophores, both from the BODIPY family, with non-overlapping excitation and emission spectra, are used so that the two populations of particles are readily distinguished in the confocal microscopy experiments, and can thus be tracked and analyzed separately.

Interactions between the polyelectrolyte brushes govern the interparticle interactions, and vary with the addition of an indifferent electrolyte to the solution. Similarly charged particles are repulsive; in a polar solvent at moderate salt concentrations, the repulsion is primarily due to the steric interaction of the brushes. Only at separation distances smaller than the Debye length, which is in the range of 1 nm in the present study, does electrostatic repulsion become important. Oppositely charged particles experience an attractive interaction; recent AFM work suggests that this attractive interaction is due to the interpenetration of the oppositely charged brushes as they form a polyelectrolyte complex.[22] The strength of the attraction is tuned by the addition of monovalent salt; at higher concentrations, the salt ions screen the interaction between the charge groups in the polymer brush, and make the formation of the polyelectrolyte complex less favorable.

We use sodium chloride as our indifferent electrolyte, and confirm that our system works as expected: similarly charged particles do not aggregate at any salt concentration up to $c \approx 1$ M, indicating that their stability is indeed due to steric interactions rather than charge repulsion. When we mix oppositely charged particles in a solution with no added salt, they aggregate strongly, whereas with an added salt concentration of around $c \approx 0.5$ M, oppositely charged particles are stable against aggregation and behave as a hard-sphere fluid. This demonstrates that the attractive interaction can be tuned by salt concentration, and is stronger at lower salt concentrations.

We expect the thickness of the polyelectrolyte brushes to govern the range of the interparticle interactions, so that the range is nearly independent of salt concentration in most of our gel experiments. The polar solvent has a dielectric constant near that of water, $\varepsilon \approx 80$–100; thus with the addition of even moderate amounts of salt, as in the experiments reported here, the screening length is on the order of $\kappa^{-1} \approx 1$ nm, and all electrostatic interactions are short-range. The thickness of the polyelectrolyte brush is a few nanometers, several times longer than the screening length, and will dominate the interaction range. Thus the salt concentration controls only the strength of the attraction between oppositely charged particles, while the repulsion between similarly charged particles and the interaction range are nearly constant over our experiments.

We use a confocal microscope (Leica SP5) to study the dynamics and the three-dimensional structure of binary mixtures of these charged colloids. The positively and negatively charged particles are imaged in separate channels, corresponding to the fluorescence emission spectra of the two fluorophores used. We obtain precise particle locations using standard algorithms to calculate the particle centroids.[23,24] To analyze the structures, we use particle locations from fully three-dimensional image stacks, while we obtain the dynamics from two-dimensional images, allowing sequential images to be taken rapidly enough to clearly track the motion of individual particles. We vary the total particle volume fraction and the strength of the attraction between oppositely charged particles to compare our results to previous work with purely attractive gels. We also vary the mixing ratio R, defined as the ratio between the number of anionic particles and the number of cationic particles in the system.

For the most deeply quenched, strongest gels, we are also able to measure the viscoelastic moduli of bulk samples. We use a stress-controlled rheometer (Anton-Paar) in a cone-plate geometry. We subject samples to a large oscillatory pre-shear in order to break up networks or large clusters formed during loading; the amplitude of this pre-shear is then gradually decreased so that no preferred direction is imposed on the final structure of the sample. The pre-sheared sample is then equilibrated for 30 minutes with a very small oscillation imposed to measure the evolution of the elastic moduli during the reformation of the gel structure. Finally, a frequency sweep is performed to measure the storage and loss moduli G' and G''.

3. Results and discussion

We begin with the symmetric case $R = 1$, in which we mix equal numbers of positively charged and negatively charged particles. At the lowest salt concentrations studied, $c = 100$ mM, and for total volume fractions in the range $\varphi_{tot} \approx 0.05$–$0.20$, the particles form a colloidal gel, a space-filling network in which particle motion is arrested. Particles aggregate into a large cluster which spans the imaging volume, and very little particle motion occurs over several minutes, with the particles executing only small fluctuations around their average positions (Fig. 1a; note that apparently disconnected clusters in the two-dimensional image are connected in the third dimension). As we decrease the strength of the attraction between oppositely charged particles by increasing the salt concentration to $c \approx 130$ mM, the space-filling network persists, but the amplitude of the particle motion increases, with larger fluctuations easily visible, and some collective motion of larger strands of the gel (Fig. 1b). With yet a further decrease in the interaction strength, at $c \approx 150$ mM, the space-filling network breaks up into a fluid of free particles and small clusters, in which the particles diffuse rapidly (Fig. 1c). (Videos available in ESI.†)

For salt concentrations in the range $c = 130$–150 mM, we also observe a transition between the gel and fluid states as we vary the total particle volume fraction φ_{tot}. At a fixed added salt concentration, we see the formation of a gel at large volume fractions, and a fluid of clusters at low volume fraction, where a spanning cluster is unable to form. These observations allows us to determine the gel line which separates the fluid region of the parameter space from the gel region, and determine the state diagram for colloidal gelation of oppositely charged particles (Fig. 2a). These symmetrically mixed binary samples with $R = 1$ show the same qualitative behavior as that established for

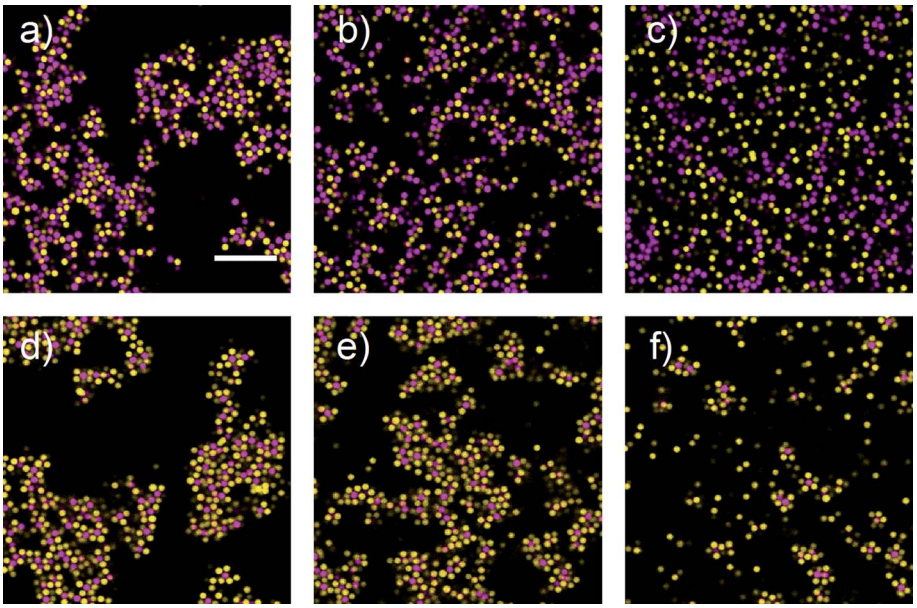

Fig. 1 Confocal images of binary mixtures of oppositely charged colloids. Negatively charged particles are shown in yellow, and positively charged particles in magenta. Interaction strength decreases in a–c, exhibiting the transition from a gel at high interaction strengths to a fluid at low interaction strengths. Mixing ratio increases in d–f, exhibiting the same transition accessed using a different tuning parameter. (a) Mixing ratio of anions to cations $R = 1$, added salt concentration $c = 100$ mM; (b) $R = 1$, $c = 130$ mM; (c) $R = 1$, $c = 150$ mM; (d) $R = 4$, $c = 100$ mM; (e) $R = 6$, $c = 100$ mM; (f) $R = 8$, $c = 100$ mM. $\varphi_{tot} \approx 0.1$ and scale bar is 20 μm for all samples.

attractive gels:[9,10,25] the formation of gels depends on both volume fraction and interaction strength, with the critical interaction strength required for gelation decreasing for higher particle volume fractions. In our system, this is manifested by the existence of gels at higher salt concentration for higher total volume fractions.

We quantify the behavior of the samples by computing the one-dimensional particle mean-square displacement over time,

$$\Delta x^2(\Delta t) = \langle (x(t + \Delta t) - x(t))^2 \rangle$$

(averaged over all particles and over all starting times t), which gives a measure of particle diffusion. In most cases, there is a clear distinction between fluid samples and gel samples, as shown in Fig. 2b. Fluids exhibit diffusive dynamics; we define fluids as samples in which the mean-square displacement increases rapidly and roughly linearly with time until the particles leave the imaging plane, indicating that the particles and clusters remain diffusive. Gels show arrested dynamics; we define gels as those samples in which the mean-square displacement reaches a plateau at long times, indicating that the particles are localized and not free to diffuse. These definitions based on measured dynamics match well with the qualitative characterizations obtained by observing the samples by eye over longer periods.

Our identifications of the strongest gels are supported by bulk rheological measurements of the storage modulus G' and loss modulus G'' (Fig. 2c). The storage modulus demonstrates a plateau at low frequency for several salt concentrations, the hallmark of a solid gel; this further confirms that these samples indeed form macroscopic sample spanning networks of aggregated colloidal particles. The moduli of weaker gels are too small to measure using the rheometer.

To better understand the nature of the gel transition, we examine the structures of the gels, and the change of these structures with interaction strength. The radial distribution function $g(r)$ provides a straightforward measure of the average structure; $g(r)$ quantifies the distribution of interparticle distances relative to a random particle distribution, highlighting correlations between particle positions. As we image positively charged (cationic) and negatively charged (anionic) particles in different spectral channels, we can distinguish between them, and calculate not only the total radial distribution function, but also the partial distribution functions for pairs of particles with similar or opposite charges. This partial radial distribution function is given by:

$$g_{ab}(r) = \frac{1}{4\pi r^2} \left\langle \frac{1}{n_b} \sum_b \delta(r - r_{ab}) \right\rangle_a$$

where each of the indices a and b indicate either positively or negatively charged particles; $\langle\rangle_a$ indicates an average over all particles of type a; n_b is the number density of particles of type b; and r_{ab} is the distance between two particles a and b.

In all gel samples, the partial $g_{-+}(r)$, indicating correlations between oppositely charged particles, shows a strong nearest-neighbor peak at about one particle diameter. In the deeply quenched cases at low salt concentration, there is also a dip after this nearest-neighbor peak, indicating a region of depletion of oppositely charged particles relative to the overall average density (Fig. 3a). In contrast, the partials $g_{++}(r)$ and $g_{--}(r)$, indicating correlations between similarly charged particles, are suppressed at one particle diameter, but have a slight, broad peak between about one and two particle diameters (Fig. 3a). This indicates that similarly charged particles are more likely to be

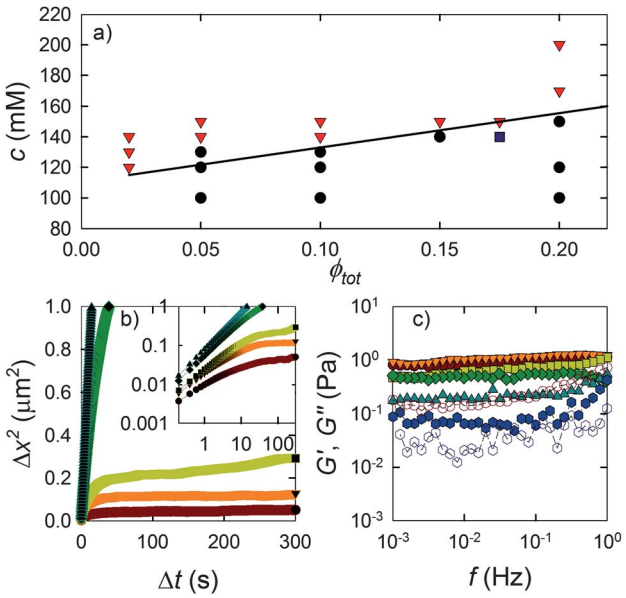

Fig. 2 (a) State diagram for the gel transition of a symmetrically mixed binary charged system; fluid samples are denoted by triangles, and gel samples by circles. The square point could not be identified as gel or fluid using the mean-square displacement criterion. The line is drawn as a guide to the eye. (b) One-dimensional mean square displacement curves for samples at several salt concentrations and $\varphi_{tot} \approx 0.05$, showing the change from arrested to diffusive behavior. From bottom to top, $c =$ 100 mM, 120 mM, 130 mM, 140 mM, and 150 mM. Inset: the same data on a log–log plot. (c) Frequency-sweep measurements for the strongest gels; solid symbols give the storage modulus G', while open symbols give the loss modulus G''. For clarity, only two examples of the loss modulus are shown. $c =$ 60 mM (circles), 80 mM (down-triangles), 90 mM (squares), 100 mM (diamonds), 110 mM (up-triangles), and 120 mM (hexagons). $\varphi_{tot} \approx 0.2$ and $\gamma = 0.1\%$ for all samples.

slightly separated but not in direct contact. The partial radial distribution functions thus suggest a typical arrangement of oppositely charged particles forming contacts, while like-charged contacts are disfavored. This local ordering persists only over short lengthscales of a few particle diameters at most, while the system is disordered at longer lengthscales. Similar results for a different system of oppositely charged particles have been reported in ref. 17. As the interaction strength between oppositely charged particles decreases, the $g_{-+}(r)$ curves flatten out toward a featureless, liquid-like curve, indicating that the particles are becoming less correlated as the gel transitions to a fluid (Fig. 3b).

Examining contacts between particles gives more local information than the sample-averaged radial distribution function. We identify contacts between particles from the microscopy data, defining two particles to be in contact if the distance between their centers falls within the first peak of $g_{-+}(r)$. Again, we identify contacts between both similarly charged and oppositely charged particles. Attractive contacts between oppositely charged particles are the bonds which allow formation of a gel network; contacts between similarly charged particles are not attractive, and so are not expected to contribute to the ability of the gel to support stress. We thus focus our attention on the attractive oppositely charged bonds. In the strongest gels at high interaction strength, a particle makes on average three bonds

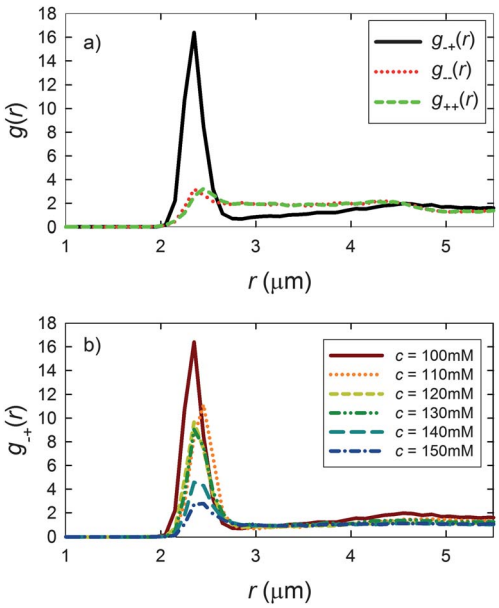

Fig. 3 (a) Partial radial distribution functions for $\varphi_{tot} \approx 0.1$ and $c =$ 100 mM. Note the large nearest-neighbor peak in the partial for oppositely charged particles, and the suppression of this peak in the partial for similarly charged particles. (b) Partial radial distribution function for oppositely charged particles at $\varphi_{tot} \approx 0.1$ as salt concentration is varied.

with oppositely charged particles. As we decrease the interaction strength, the contact number distribution shifts to lower values, as shown in Fig. 4a; the gel line is crossed when the average bond number falls below about 1.

This trend is in clear contrast to the case of purely attractive gels, in which stronger gels tend to be more chain-like with fewer contacts, while weaker gels closer to the gel line have thicker strands and more contacts, as shown in Fig. 4b (data taken from ref. 3; see also ref. 2). In strong attractive gels, a particle attaching to the gel is unable to rearrange, so that the structure of the gel is essentially determined by chance contact events. In contrast, lower interaction strengths allow particle rearrangements within the gel; since all contacts are attractive, it is favorable for

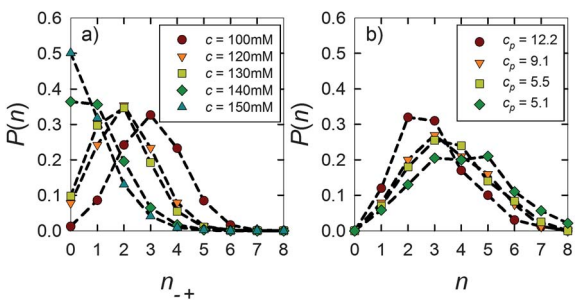

Fig. 4 (a) Distribution of number of cationic contacts of anionic particles in a binary gel as interaction strength is changed. $\varphi_{tot} \approx 0.1$ for all samples. (b) Distribution of number of contacts in a purely attractive gel as interaction strength is changed. Data taken from ref. 3 with permission of the authors and IOP. $\varphi = 0.03$ for all samples. The labels c_p refer to the concentration of polymer depletant in mg mL^{-1}, and are numerically roughly equivalent to the depth of the attractive well in kT (see ref. 3).

particles to form as many contacts as possible, and so rearrangement leads to higher contact numbers.[3]

We suggest that in binary gels, local rearrangements are not likely to result in more favorable contacts. Essentially this is because triangles in the binary gel are not favored. In a purely attractive gel, a triangle consisting of three particles in mutual contact involves three attractive bonds; however, in the binary gel, such a triangle involves only two attractive bonds between oppositely charged particles, the third contact being a repulsive contact between similarly charged particles. This is a type of geometric frustration which in part gives rise to the complexity and richness of the system. Thus triangles do not tend to form in binary gels, and as the interaction strength decreases and particles are more able to rearrange, they are not able to form additional favorable contacts. We suggest that instead, several particles of one charge all contacting the same oppositely charged particle will tend to spread out around that central particle as far from one another as possible. We do not expect this to be due to charge repulsion, as the short screening length ensures that any charge interactions are very short-range. Rather, the arrangement of the particles farther from each other is likely to be simply an entropic effect. This spreading out blocks other particles from contacting the central particle, thus lowering the average contact number. The lower interaction strength may also allow particles to more readily detach from the gel, making the gel structure more sparse and decreasing the typical contact number within the gel. In a binary gel, in contrast to an attractive gel, the gel line is approached as particles in the gel are no longer able to form enough favorable contacts to sustain a network.

Another striking difference between this binary system and an attractive system is the ability to vary the mixing ratio R of the two particle species. The behavior of the system changes dramatically with mixing ratio, even as the total volume fraction of particles and the added salt concentration are held constant. For a total particle volume fraction of $\varphi_{tot} \approx 0.10$ and an added salt concentration $c \approx 100$ mM, a sample at $R = 1$ with an equal number of anionic and cationic particles forms a strong gel, with the particles fluctuating over only a small localization length (Fig. 1a). With an excess of anionic particles at ratios up to $R = 6$, the amplitude of particle motion increases, as the particles fluctuate farther from their equilibrium positions (Fig. 1d and e). As the mixing ratio increases further to $R = 8$, the gel breaks up into smaller clusters which are able to move freely (Fig. 1f). Each of these clusters contains several cationic particles coated by excess anionic particles. As the exteriors of these clusters present only anionic particles, the clusters cannot aggregate together into a spanning gel network. The critical mixing ratio for gelation with this high interaction strength is between $R = 6$ and $R = 8$. This is similar to the critical minority number fraction $x \approx 0.15$, corresponding to a mixing ratio of $R = 1/x - 1 \approx 5.7$ reported in simulations for irreversible bonds.[26] As interaction strength decreases, this critical mixing ratio becomes lower (Fig. 5).

We consider the structure of these asymmetrically mixed gels by again examining the contact-number distributions. With a larger and larger excess of anionic particles, it is the cationic particles bound to a single anionic particle that become the most relevant contacts to the formation of a gel. Essentially the gel consists of cationic particles bound together by anionic particles; an anionic particle is only part of the skeleton of the gel if it

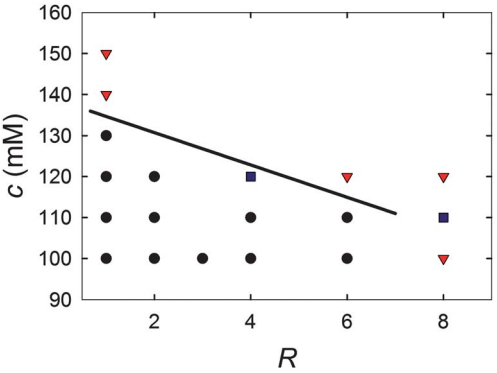

Fig. 5 State diagram showing the gel transition of the oppositely charged system at fixed total volume fraction ($\varphi_{tot} \approx 0.1$); fluid samples are denoted by triangles, and gel samples by circles. The square points could not be identified as gel or fluid using the mean-square displacement criterion. The line is drawn as a guide to the eye.

makes at least two attractive bonds to cationic particles. The number of anionic particles bonded to a cationic particle is less important, as many of those excess anionic particles will not form an additional attractive bond. As the excess of anionic particles increases, the distribution of n_{-+}, the number of cationic particles bonded to an anionic particle, shifts to lower bond numbers (Fig. 6a). The gel line is reached approximately when the average n_{-+} falls below 1.

It is also interesting to note what happens to the distribution of n_{+-}, the number of excess anionic particles bonded to a given cationic particle. As the asymmetry increases, so that there is a greater excess, it is unsurprising that the distribution shifts to a cationic particle having more anionic particles bonded to it (Fig. 6b). What is unexpected is that this distribution appears to reach a saturation at high asymmetry, with the distributions for $R = 6$ and $R = 8$ appearing quite similar. This saturation coincides with the gel line. This suggests that part of the reason for the concurrent decrease in the number of cationic particles contacting anionic particles is that the cationic particles become overcrowded with anionic particles. At high asymmetries, a typical cationic particle is surrounded by sufficient anionic particles that there is no opportunity for another anionic particle to make contact. If none of the anionic neighbors is in contact with another cationic particle, there will be no opportunity for a structure-supporting bond to be formed; the cluster consisting of the cationic particle and its surrounding shell of anionic particles will remain stable and not become part of a larger cluster. This situation is analogous to the formation of soluble complexes in the coacervation of oppositely charged polymers.[27] The saturation drives the number of cationic particles that can contact one anionic particle below the critical number for gelation. It remains an interesting question whether the distribution truly saturates below complete coverage, or reaches a close-packed arrangement as the system approaches an infinitely large mixing ratio.

The trends of contact number distributions with mixing ratio remain similar as the interaction strength decreases. At salt concentrations of $c = 110$ mM and $c = 120$ mM, the mean numbers of cationic particles contacting an anionic particle again decrease with increasing mixing ratio (Fig. 6c and e). Again we observe that the gel line coincides with a mean bond number of

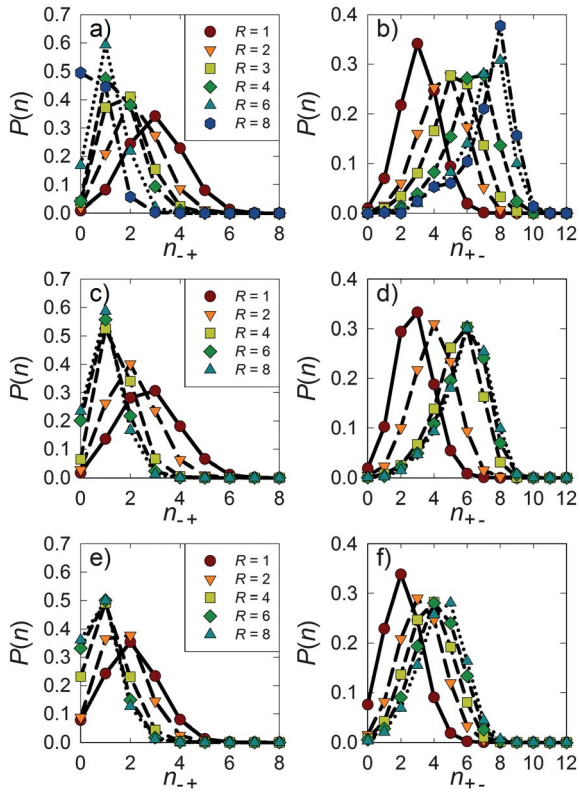

Fig. 6 Distribution of the number of positively charged contacts of negatively charged particles (a, c and e), and negatively charged contacts of postively charged particles (b, d and f) as the mixing ratio R is changed. a and b: $c = 100$ mM; c and d: $c = 110$ mM; e and f: $c = 120$ mM. Note that the trends in a, c, and e are similar to that in Fig. 4a, while in b, d, and f, there seems to be an approach to a saturated distribution at the highest asymmetry. All samples at $\varphi_{tot} \approx 0.1$.

about 1, although the transition occurs at a different mixing ratio (Fig. 7).

The trend of anionic contacts of cationic particles is also the same at different interaction strengths, reaching a saturation distribution which is shifted to lower contact numbers as interaction strength decreases (Fig. 6d and f). The mean contact number at a mixing ratio of $R = 8$ is above 7 for a high interaction strength at $c = 100$ mM, but decreases to about 6 at $c = 110$ mM and is less than 4.5 for $c = 120$ mM (Fig. 7). This supports our earlier observation that particles form fewer oppositely charged contacts at lower interaction strengths; this is robust even when there is a large excess of one type of particles. Thus as the interaction strength decreases, the gel weakens not simply because of the weakening of the individual bonds, but because of the reduction in the number of attractive bonds in the gel. This provides a stark contrast to purely attractive gels where failure of individual bonds to carry a stress is the sole cause of instability of the gel at the gel point. We further note that the distribution of contacts between two anionic particles also shifts to lower numbers at higher salt concentrations (data not shown), supporting again the argument that the long-range separation of like charges is not due to charge effects; the screening of charge repulsion would allow more such contacts at high salt concentrations rather than fewer.

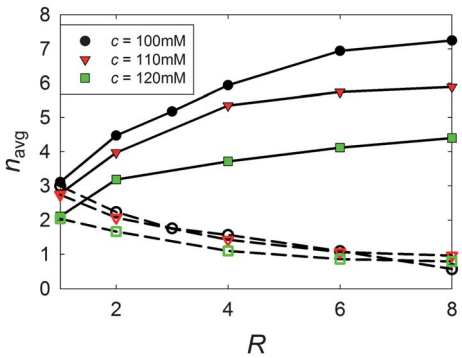

Fig. 7 Mean number of contacts to oppositely charged particles as a function of mixing ratio, for several salt concentrations. The lower branches (open symbols, dashed lines) show the average number of cationic particles bonded to an anionic particle; the gel line in all cases is reached at a mean contact number of about 1. The upper branches (filled symbols, solid lines) show the average number of anionic particles bonded to a cationic particle; note the apparent saturation to a plateau, with the saturation value depending on interaction strength. All samples at $\varphi_{tot} \approx 0.1$.

4. Conclusion

We have introduced a novel experimental model system of oppositely charged colloidal particles which allows a detailed study of colloidal gelation in the presence of a mixture of attractive and repulsive interparticle interactions, and identified a novel mechanism underlying the formation and structure of these binary colloidal gels. The most striking difference between oppositely charged colloidal gels and purely attractive gels is that in the binary case, there appears to be a critical mean bond number of 1 for gelation, which is the same no matter how the gel line is approached. We observe this critical mean bond number in symmetric gels as the interaction strength varies, and in asymmetric gels as mixing ratio varies at several different interaction strengths. With variation of either tuning parameter, particles tend to form fewer structure-supporting bonds as the gel line is approached. Thus over a range of parameters, the presence of a gel correlates with the mean number of attractive bonds a particle makes: if this mean bond number is greater than one, a gel will form, while if it is less than one, the system will form a fluid of clusters.

The similarity in the effects of two very different tuning parameters emphasizes that the structural integrity of a binary gel is determined by the contacts between oppositely charged particles; not all possible particle contacts are favorable or contribute to the ability of the gel to bear stress. This is in clear contrast to the case of purely attractive gels, in which any particle contact stabilizes the gel. In binary gels, unlike in purely attractive gels, rearrangements do not allow for a significant increase in the number of favorable contacts. With a decrease in the interaction strength, particles are more able to rearrange to form string-like structures and are more able to detach from the aggregate, leading to lower contact numbers; with an increase in the mixing ratio, excess particles of one type saturate the minority particle type, preventing further attractive bonds from forming. Either tuning parameter affects the number of attractive bonds, and if this number is below a critical average of about 1, a gel cannot form.

While polyelectrolyte brushes present an interesting and relevant system, they are not the only method of introducing opposite charges on colloidal particles, and it remains an interesting question how the particulars of the interaction might affect our results. Our gels appear to be similar in structure to those formed by oppositely charged particles more nearly described by a bare surface charge with a screened Coulomb or Yukawa interaction,[18,28] suggesting some generality to our results, but we cannot rule out that some details may differ. We expect the interpenetration of the polyelectrolyte brushes to pose a kinetic barrier to the rotation of bonds between oppositely charged particles; we can speculate that this barrier may change in the case of bare surface charges, changing the ability of the particles to rearrange within the gel. The range of the interaction also plays a role in determining the internal gel structure; for example, in experiments with longer-range interactions, the gel strands became locally crystalline,[28] which we did not observe in our short-range system. A related question well worth further investigation is whether the onset of gelation of oppositely charged colloids is generally driven by a thermodynamic phase separation. In a purely attractive system, gelation appears to be a consequence of arrested gas–liquid spinodal decomposition.[25] Simulations have indicated that spinodal decomposition also drives gelation in a system of oppositely charged particles interacting *via* a Yukawa potential.[18,28] We see nothing to suggest that the onset of gelation in our system is not also driven by a thermodynamic phase transition, although we are unable to confirm whether this is the case, due to the difficulty of calculating the equilibrium phase diagram. The relationship between the gel state and the equilibrium phases of this system invites further study.

The binary system of oppositely charged colloidal particles introduced here constitutes a new system valuable for studying a range of new phenomena in gelation which have not been observed in purely attractive gels, and which may bear on other examples of gelation and aggregation driven by opposite electric charges. These binary gels offer the novel parameter of the mixing ratio of the two particle species, which can be used to tune the system between a fluid and a gel, and to control the structure of the gels. Furthermore, we see that the structure of binary gels tends toward lower contact numbers on approach to the gel line whether interaction strength or mixing ratio is varied, in contrast to the opposite trend exhibited in attractive gels. The mechanism of gel formation in a binary gel is thus distinct from that in an attractive gel.

Acknowledgements

Many thanks to Katharine Jensen for the use of her particle tracking code and advice on locating particles. This material is based upon work supported by the NSF through the Graduate Research Fellowship (DGE-0946799 and DGE-1144152; E.R.R.), DMR-1006546, and the Harvard MRSEC (DMR-0820484).

References

1 A. I. Campbell, V. J. Anderson, J. S. van Duijneveldt and P. Bartlett, *Phys. Rev. Lett.*, 2005, **94**, 208301.
2 C. J. Dibble, M. Kogan and M. J. Solomon, *Phys. Rev. E: Stat., Nonlinear, Soft Matter Phys.*, 2006, **74**, 041403.
3 A. D. Dinsmore and D. A. Weitz, *J. Phys.: Condens. Matter*, 2002, **14**, 7581–7597.
4 A. D. Dinsmore, V. Prasad, I. Y. Wong and D. A. Weitz, *Phys. Rev. Lett.*, 2006, **96**, 185502.
5 A. H. Krall and D. A. Weitz, *Phys. Rev. Lett.*, 1998, **80**, 778–781.
6 S. Manley, H. M. Wyss, K. Miyazaki, J. C. Conrad, V. Trappe, L. J. Kaufman, D. R. Reichman and D. A. Weitz, *Phys. Rev. Lett.*, 2005, **95**, 238302.
7 W. C. K. Poon, A. D. Pirie and P. N. Pusey, *Faraday Discuss.*, 1995, **101**, 65.
8 P. N. Pusey, A. D. Pirie and W. C. K. Poon, *Phys. A*, 1993, **201**, 322–331.
9 P. N. Segrè, V. Prasad, A. B. Schofield and D. A. Weitz, *Phys. Rev. Lett.*, 2001, **86**, 6042–6045.
10 V. Trappe and P. Sandkühler, *Curr. Opin. Colloid Interface Sci.*, 2004, **8**, 494–500.
11 V. Trappe and D. A. Weitz, *Phys. Rev. Lett.*, 2000, **85**, 449–452.
12 E. Zaccarelli, *J. Phys.: Condens. Matter*, 2007, **19**, 323101.
13 A. Mohraz, E. R. Weeks and J. A. Lewis, *Phys. Rev. E: Stat., Nonlinear, Soft Matter Phys.*, 2008, **77**, 060403(R).
14 M. M. van Schooneveld, V. W. A. de Villeneuve, R. P. A. Dullens, D. G. A. L. Aarts, M. E. Leunissen and W. K. Kegel, *J. Phys. Chem. B*, 2009, **113**, 4560–4564.
15 M. Cerbelaud, A. Videcoq, P. Abélard, C. Pagnoux, F. Rossignol and R. Ferrando, *Soft Matter*, 2010, **6**, 370.
16 M. A. Piechowiak, A. Videcoq, F. Rossignol, C. Pagnoux, C. Carrion, M. Cerbelaud and R. Ferrando, *Langmuir*, 2010, **26**, 12540–12547.
17 M. S. Romero-Cano, J. B. Caballero and A. M. Puertas, *J. Phys. Chem. B*, 2006, **110**, 13220–13226.
18 E. Sanz, M. E. Leunissen, A. Fortini, A. van Blaaderen and M. Dijkstra, *J. Phys. Chem. B*, 2008, **112**, 10861–10872.
19 E. Spruijt, H. E. Bakker, T. E. Kodger, J. Sprakel, M. A. Cohen Stuart and J. van der Gucht, *Soft Matter*, 2011, **7**, 8281.
20 T. E. Kodger, R. Guerra, J. Sprakel and D. A. Weitz, unpublished work.
21 H. Sedgwick, S. U. Egelhaaf and W. C. K. Poon, *J. Phys.: Condens. Matter*, 2004, **16**, S4913–S4922.
22 E. Spruijt, M. A. Cohen Stuart and J. van der Gucht, *Macromolecules*, 2010, **43**, 1543–1550.
23 Y. Gao and M. L. Kilfoil, *Opt. Express*, 2009, **17**, 4685.
24 J. C. Crocker and D. G. Grier, *J. Colloid Interface Sci.*, 1996, **179**, 298–310.
25 P. J. Lu, E. Zaccarelli, F. Ciulla, A. B. Schofield, F. Sciortino and D. A. Weitz, *Nature*, 2008, **453**, 499–503.
26 J. M. López-López, A. Schmitt, A. Moncho-Jordá and R. Hidalgo-Álvarez, *Soft Matter*, 2006, **2**, 1025.
27 J. van der Gucht, E. Spruijt, M. Lemmers and M. A. Cohen Stuart, *J. Colloid Interface Sci.*, 2011, **361**, 407–422.
28 E. Sanz, C. Valeriani, T. Vissers, A. Fortini, M. E. Leunissen, A. van Blaaderen, D. Frenkel and M. Dijkstra, *J. Phys.: Condens. Matter*, 2008, **20**, 494247.